International journal of advances in engineering and management (IJAEM)
Volume 3, issue 6 June 2021, pp: 1822-1832 www.ijaem.net ISSN: 2395-5252

Production Technology of Graphene

Tarun Radadiya

Researcher &PG Data Science Student of Amity University (India), Student of eCornell University (USA), Team Lead in Paytm

Submitted: 05-06-2021 Revised: 18-06-2021 Accepted: 20-06-2021

ABSTRACT : Graphene wonder and amazing material in the universe. Graphene all the excellent properties mechanical, optical, electrical, chemical, thermal, magnetic, electronics. This reasongraphene is one of the material uses all application like tissue engineering, bio imaging, Polymerase chain reaction, devices, drug deliver, biomicrorobotics, testing, electronics, transistors , transparent conducting electrode , frequency multiplier, optoelectronics, hall effect sensors, quantum dots, organic electronics, light processing, optical modulator,infrared light detection, energy, generation,ethanol distillation, solar cell, fuel cell, storage, super capacitor, Electrode for Li-ion batteries,Hydrogen storage,Rechargeable battery,Sensors,Molecular adsorbtion,Piezoelectric effect,Body motion,Environmental,Contaminant removal,Water filtration,Plasmonics and metamaterials,Lubricant,Radio wave absorption,Redox,Nanoantennas,Sound transducers,Waterproof coating,Coolant additive,Reference material,Thermal management, Structural material,Catalyst, power electronics, power transmission system , biomedical. Graphene is most important point of production required different application and different technology using high quality production of the graphene.

Keyword:graphene properties, application, fabrication of graphene, fabrication technology

INTRODUCTION

Graphene become the next disruptive technology, replacing some of the currently used materials and leading to new markets. Is it versatile enough to revolutionize many aspects of our life simultaneously? In terms of its properties, graphene certainly has the potential. Graphene is the first two-dimensional (2D) atomic crystal availableto us. A large number of its material parameters such as graphene reported so far include high values of its Young's modulus (~1,100 GPa)[1], fracture strength (125 GPa)[1], thermal conductivity (~5,000 W $m^{-1}K^{-1}$)[2], mobility of charge carriers (200,000 $cm^2V^{-1}s^{-1}$)[3]and specific surface area (calculated value, 2,630 m^2g^{-1})[4], plus fascinating transport phenomena such as the quantum Hall effect[5], field-effect mobilities as high as 15 000 cm^2/Vs and carrier velocity of ~108 cm/s at room temperature [6].Graphene is composed of sp^2 bounded carbon atoms arranged in two-dimensional honeycomb lattice. The lattice can be seen as consisting of two interpenetrated triangular sub lattice, for which the atoms of one sub lattice are at the center of the triangular defined by other with carbon to carbon inter atomic length, ac-c, of 1.42Å.the unit cell comprises two carbon atoms and is invariant under a rotation of 120° around any atom. Each atom one as orbital and two in plan p orbital's contributing to the mechanical stability of the carbon sheet. The remaining p orbital, perpendicular oriented to the molecular plan, hybridizes to from the conduction and valence band, which dominate planer conduction phenomena [7].

Structural composites and so on and so forth. Its fascinating attributes have triggered an avalanche of research publications and patent

Filings. The industry, private investorsand governments, are providingsubstantial funding in grapheneresearch and innovation, which will

help in accelerating the pace of itscommercialization. USA, Europe,Korea, UK, Japan and other Asiancountries are investing a largeamount of financial capital. It isexpected that the market forgraphene would grow by leaps andbounds in the coming decade.According to the latest report"Graphene: Technologies,Applications and Markets" releasedby BCC the global graphene market

is projected to grow to $67 million in2015 and $675.1 by 2020 at aCompound Average Annual GrowthRate (CAGR) of 58.7% within aperiod of 5 years. Another reportentitled "world market for grapheneto 2017" by the future markets, Inc.2011 estimates that the productionvolume of graphene in 2010 was 28tonnes and is projected to grow to573 Tonnes-2017.Graphene is undoubtedly emerging as the most promising nanomaterial because of its unique combination of superb properties, which opens a way for its exploitation in a wide spectrum of applications. However, it has

International journal of advances in engineering and management (IJAEM)
Volume 3, issue 6 June 2021, pp: 1822-1832 www.ijaem.net ISSN: 2395-5252

to overcome a number of obstacles before we can realize its full potential for practical applications. One of the greatest challenges being faced today in

Table 1Graphene Synthesis Methods

Micromechanical Exfoliation **Flakes (5Flakes to 100µm)**	Carbon Nanotube Unzipping **Nan ribbons (fewmicrons)**	Liquid Phase Exfoliation **Nan sheets (nm to a few µm)**	Epitaxial Growth on SiC **Thin films (>50 µm)**	Chemical Reduction of Graphite Oxide **Nanoflakes/Powder (nm to a few µm)**	CVD (on, Ni, Cu, Co) **Thin film (<75cm)**
Research Purpose	Interconnects FETs NEMs Composites	Polymer Fillers Transparant Electrodes Conductive Paints Sensors	Transistors Circuits Interconnects Memory Semiconductors	Polymer Fillers Battery Electrodes Supercapacitors Conductive Inks & Paints Sensors	Touch Screens Smart Windows Flexible LCDs & OLEDs Solar Cells
Small Scale Production High Cost High Quality Uneven Films	Moderate Scalibility High Yield High Quality Potentially Low Cost	High Scalability Low Yield Moderate Quality Low Cost Impure	Low Yield High Cost High Quality High Process Temperature (15000C) Very Expensive Substrate	High Scalability Low Cost Low Purity High Defect Density	Moderate Scalability High Cost High Quality High Process Temparature (>1000oC)

Commercializing graphene is ho graphene is how to produce high quality material, on a large scale at low cost, and in a reproducible manner [8].

Fabrication of a Graphene MoS2 Junction
Micromechanical Exfoliation

Graphite is a highly anisotropic material made of weakly coupled layers of carbon atomsbonded in a hexagonal lattice. Its building-block, an isolated single atomic layer (monolayer) calledgraphene, is only recently accessed experimentally [9-14]. Although the stacking of graphene layersis only supported by a weak interlayer coupling, the electronic properties change dramatically forthe monolayer graphene as compared to the bulk graphite. As graphene is a new nano-material withunusual electronic properties, its electronic, optical, thermal and other properties have not beenstudied completely yet [15-19]. Knowledge of how these properties evolve from monolayer grapheneto graphite will facilitate the development of graphene devices. In particular, optical detection relying on light scattering is especially attractive, because it is fast, sensitive, andNon-destructive. Raman scattering has recently emerged as a viable, non-destructive technique forthe identification of mono- and few layer graphene [20-23].

Currently, graphene is prepared by different methods such as mechanical exfoliation of graphite using scotch tape [10], chemical exfoliation of graphite [11], epitaxial growth of graphene bythermal graphitization of SiC [20], chemical vapor deposition of hydrocarbon gases on transitionmetals [21], exfoliation of graphite by sonication [22], etc. However, at present there is no idealmethod for synthesizing defect free graphene sheets. Detailed understanding of growth kinetics andproduction control is highly desired to prepare large-scale high quality graphene. Disadvantages ofthe mechanical exfoliation (cleavage) or Scotch tape method, which is the first method of obtainingtwo-dimensional crystals, are small surface area of monolayer graphene obtained [23].

Graphene samples are synthesized by Scotch tape method, identified by optical microscopy, and characterized then by Raman spectroscopy and AFM. For synthesizing graphene samples, oxidized Si wafers (with areas of ~1×1 cm^{-2}, thickness of 525 µm and resistivity of0.001–0.005 Ωcm) are used. The thickness of SiO2 on the top of Si substrate was 300 nm.The Raman spectra are measured by WITec Alpha300 Raman system (spectral resolution ofspectrometer is 1 cm^{-1}) using a laser excitation of 632.6 nm, 514.5 nm and 487.9 nm (with a triplefrequency He-Ne and Ar lasers as

International journal of advances in engineering and management (IJAEM)
Volume 3, issue 6 June 2021, pp: 1822-1832 www.ijaem.net ISSN: 2395-5252

excitation source) delivered through a single-mode optical fiber,whose spot size is limited by the diffraction. Using a long working distance focusing objectivelenses (10× and 100×) with numerical apertures NA =0.90 and 0.80, the spot size of about500 nm is obtained. With an incident light power of 0.2mW, heating effects can be neglected. TheRaman spectra are measured using a grating with 1800 g'mm and a solid state cooled CCD detector.The Raman spectra of as-prepared and elaborated monolayer graphene samples with different areaswere recorded under the same experimental conditions. The topography and height profiles ofgraphene samples are obtained by non-contact AFM.

Graphene samples are prepared by Scotch tape method, which is the following [20]. Graphene is produced by micromechanical cleavage or exfoliation (repeated peeling) of highly oriented pyrolytic graphite by the scotch tape, i.e. slicing this layered material by gently rubbing it against another surface on the scotch tape. After that, it is transferred to an oxidized silicon wafer coveredwith SiO2 layer with thickness of 300 nm. Under an optical microscope with a 50× or 100×objective lens, it is possible to see plenty of thick and tiny flakes of graphite on Si'SiO2 wafer:large, shiny pieces of all kinds of shapes and colors (Figure.1a). The optical images of as-preparedgraphene samples with different magnification obtained after micromechanical cleavage of bulkgraphite are shown in Fig.1. It is possible to observe monolayer graphene: highly transparent,crystalline shapes having little color compared with the rest of the substrate (Figure.1b). The ability tocreate graphene with such a simple procedure ensures that graphene was produced an uncountable number of times since graphite was first mined and the pencil invented in 1565.

After preparation of the graphene samples the identification of graphene layers is still aserious obstacle. It is extremely difficult to find small graphene pieces in the haystack of millions ofthicker graphitic flakes, which appear during the cleavage (Figure.1a). For that reason at the beginning the surface of graphene carefully scanned in an optical microscope, which allows distinguishingmono- or few-layer graphene from bulk graphite. With the thickness of 300 nm of SiO2 cap layer,the ultrathin graphitic flakes get visible with an optical microscope. Few layer graphene flakes are sufficiently transparent to add to an optical path, which changes their interference color with respectto an empty substrate. For a certain thickness (300 nm) of SiO2 layer, even a monolayer was foundto give sufficient contrast to differentiate graphene layers among thicker flakes scattered over asubstrate. These layers have a slightly different color in the optical microscope (Figure.1b). It appearsthat darker color corresponds to thicker sample. The color of much thicker layers (more than 10layers) does not follow this trend and can change from blue to yellow and then to gray (Figure.1a) [24].

Micromechanical exfoliation of graphene using PDMS stamps

International journal of advances in engineering and management (IJAEM)
Volume 3, issue 6 June 2021, pp: 1822-1832 www.ijaem.net ISSN: 2395-5252

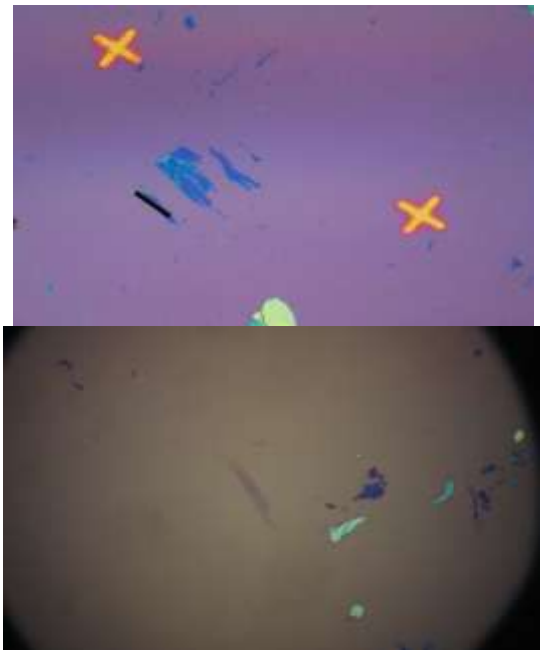

Figure: -1(a)(b). Optical images of monolayer graphene with 10× and 100× magnification

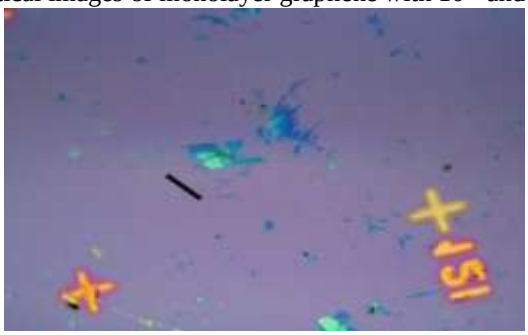

Figure: - 2 (A) MoS_2 fabricated via PDMS stamping on a 300 nm Si/SiO_2 substrate. Scale bar is 20 μm in length.B) MoS_2 also fabricated via PDMS stamping, but on a 285 nm Si/SiO_2 substrate.

In order to isolate MoS_2, PDMS stamping was used instead of micromechanical exfoliation, due to the fact that the micromechanical exfoliation process tears apart the more brittle flakes of MoS_2, making it difficult to isolate a large-area, single-layer flake. A bulk flake of MoS_2 is first exfoliated on a piece of blue tape so that the flakes do not break apart as fast as they do on clear tape. The amount of MoS_2 on the tape is kept very dense, to allow for maximum deposition. A clean, prepared stamp of PDMS, roughly 2 x 2 cm is then placed on the tape, and pulled off quickly to grab the most pieces. This stamp is then positioned over the Si/SiO_2 wafer, where it is pressed for roughly 30 seconds. Then the stamp is slowly removed so that many thick pieces will be taken off, but thinner ones will remain. This wafer is then taken to an optical microscope where pieces of MoS_2 that are good candidates for substrate transfer are identified. Good candidates for transfer are flakes that look to be large enough in area (>70 microns) to use in a prefabricated transistor device, but also thin enough for either laser-thinning or direct deposition

A PDMS stamping technique was used to simultaneously thin and deposit MoS_2. A PDMS stamp, with MoS_2 deposited on it, was placed on a Si/SiO_2 wafer. As shown in Figure 2, thin layers of MoS_2 can be isolated using this technique. Figure 2A depicts a few multilayered flakes that are about 10-13 layers thick on a 300 nm Si/SiO_2 substrate. Figure 2B is more multilayered flakes of about the same thickness, but on a 285 nm Si/SiO_2 substrate. In both of these pictures, the crosshairs are alignment markers that are used to relocate samples after they have been identified. While this method is limited in the size of the area we can stamp, it can produce good candidates for our prospective device.

International journal of advances in engineering and management (IJAEM)
Volume 3, issue 6 June 2021, pp: 1822-1832 www.ijaem.net ISSN: 2395-5252

Raman Spectroscopy and Laser Thinning.

A Thermo DXR Raman spectrometer was used to perform Raman shift measurements on both graphene and MoS_2 samples. A laser of 532 nm with a normal resolution grating of 900 lines/micron is used at a power of between 0.1 and 3 mW for Raman shift measurements, and a power of 10 mW for laser thinning. The laser thinning procedure described by Castellanos-Gomez et al was used as a building block for this technique, with some slight alterations. [25] The same Raman spectrometer mentioned above was used to perform the laser thinning, so that there could bein situ experimentation and characterization. The thinning was conducted by finding a flake of MoS_2 that looked to be less than 7-10 layers thick (characterized under the microscope visually by having a slight light-bluish tint). Then a Raman map was used so that there could be laser impaction at the smallest resolution of this instrument (1 micron). Therefore, a flake that was 10x10 microns would have a 100 point grid overlaid on it. At each point three exposures were taken, each lasting 0.5 seconds, with a maximum laser power of 10 mW. After the map was taken, a sample spectrum could be obtained to examine the effect of the thinning; the thinning could also be verified with optical means.

Raman spectroscopy has been used to determine the number of layers and existence of two-dimensional materials since their inception [20]. When looking at the output of a Raman spectrum, a few things must be considered, chiefly what the spectrum should look like in context. For graphene, the relative intensities of the G (~1580 cm^{-1}) and G' (~2700 cm^{-1}) peak are most important. The difference in intensities between these two peaks can roughly tell how many layers are being looked at. MoS_2 is not so simple; the relative intensities are of very little importance to the number of layers. The most telling characteristic of the Raman spectrum of MoS_2 is the difference between the two peaks of few-layer MoS_2. As the two peaks shift towards each other, a difference of around 20 cm-1 is ideal for single-layer MoS_2.

A thin flake of MoS_2, such as that shown in Figure 2, was then bombarded with a laser to etch away additional layers. A Raman spectrophotometer can be used to do this procedure, and also characterize itin situ. Raman spectra taken from the MoS_2 being laser-thinned were compared to quantify how much material is removed from the top of the target flake. The three Raman spectra in Supplemental Figure 1 represent the spectra taken before laser thinning, and after each treatment. It can be seen that as more treatments are applied to the sample, the two peaks near the right end of the spectrum shift toward each other, this is characteristic of few layer MoS_2, and can also help us in quantifying the change innumber of layers between treatments [26].

Carbon Nanotube Unzipping Graphene Nanoribbons

Graphene, or single-layered graphite, with its high crystallinity andinteresting semimetal electronic properties, has emerged as anexciting two-dimensional material showing great promise for thefabrication of nanoscale devices[27-29]. Thin, elongated strips ofgraphene that possess straight edges, termed graphene ribbons,ngradually transform from semiconductors to semimetals as theirwidth increases[30-33], and represent a particularly versatile variety ofgraphene. Several lithographic[33,34] chemical[35-37] and synthetic[38]procedures are known to produce microscopic samples of graphenenanoribbons, and one chemical vapour deposition process[39] hassuccessfully produced macroscopic quantities of nanoribbons at950 6C. Here we describe a simple solution-based oxidative processfor producing a nearly 100% yield of nanoribbon structures bylengthwise cutting and unravelling of multiwalled carbon Nanotube (MWCNT) side walls. Although oxidative shortening ofMWCNTs has previously been achieved [40], lengthwise cutting ishitherto unreported. Ribbon structures with high water solubilityare obtained. Subsequent chemical reduction of the Nanoribbonsfrom MWCNTs results in restoration of electrical conductivity.These early results affording nanoribbons could eventually leadto applications in fields of electronics and composite materials where bulk quantities of nanoribbons are required [41-43].

International journal of advances in engineering and management (IJAEM)
Volume 3, issue 6 June 2021, pp: 1822-1832 www.ijaem.net ISSN: 2395-5252

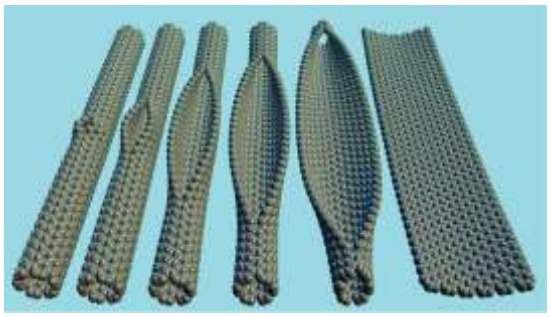

Figure: - 3Nanoribbon formation and imaging. (a) Representation of the gradual unzipping of one wall of a carbon nanotube to form a nanoribbon.

The mechanism of opening is based on previous work on the oxidation of alkenes by permanganate in acid. The proposed first step in The process is manganate ester formation (2, Figure 3b) as the ratedeterminingstep, and further oxidation is possible to afford thedione (3, Figure. 3b) in the dehydrating medium[44]. Juxtaposition of thebuttressing ketones distorts the b,c-alkenes (red in 3), making themmore prone to the next attack by permanganate. As the processcontinues, the buttressing-induced strain on the b,c-alkenes lessensbecause there is more space for carbonyl projection; however, thebond-angle strain induced by the enlarging hole (or tear if originatingfromthe end of the nanotube) would make the b,c-alkenes (4, Figure. 3b)increasingly reactive. Hence, once an opening has been initiated, itsfurther opening is enhanced relative to an unopened tube or to anuninitiated site on the same tube. The ketones can be further converted, through their O protonated forms, to the carboxylicacids[45] that will line the edges of the nanoribbons. Finally, relief ofthe bond-angle strain when the nanotube opens to the grapheneribbon (5, Figure. 3b) slows further dione formation and cutting[44].Thus, the preference for sequential bond cleavage over randomopening and subsequent cutting, as occurs with nitric acid oxidation,can be explained by concerted attachment to neighbouring carbonatoms by permanganate, contrasting with the random attack on nonneighbouringcarbon atoms by the nitroniumspeciesfromnitric acid.The surface of the now-less-strained nanoribbon remains prone to1,2-diol formation, which leads to the overall highly oxidized ribbon,but this is less likely to result in further oxidative cutting to the dioneowing to relief of the tubular strain on the double bonds.We achieved the same unzipping process in single-walled carbonnanotubes (SWCNTs), to produce narrow nanoribbons, but theirsubsequent disentanglement is more difficult.

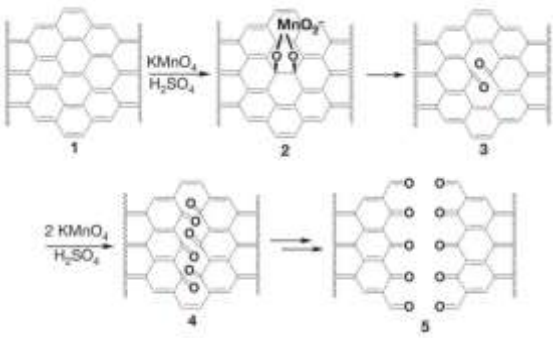

Figure :-3Nanoribbon formation and imaging.
(b)The proposed chemical mechanism of Nanotube unzipping.

We used transmission electron microscopy (TEM), atomic force microscopy (AFM) and scanning electron microscopy (SEM) toImage the ribbon structures. TEM analysis shows Nanoribbons (Figure. 1c) produced from MWCNTs with a starting diameter of 40–80nm and approximately 15–20 inner nanotube layers (additional TEM images of untreated MWCNTs can be found in the Supplementary Figure. 3a, b). After reaction, the width of the carbon nanostructures increased to.100nm and they had linear edges with little pristine MWCNT side-wall

International journal of advances in engineering and management (IJAEM)
Volume 3, issue 6 June 2021, pp: 1822-1832 www.ijaem.net ISSN: 2395-5252

structure remaining (seeSupplementary Figure 3). The MWCNTs used were produced from a chemical vapour deposition process22; we attempted the same H2SO4–KMnO4 treatment on a single sample of laser-oven-produced MWCNTs, but fewer nanoribbon-like structureswere detected. AFM imaging (Figure. 1d) shows the presence of single atomic layers after tip sonication of the solution for 30 min to yield well-dispersed and sonication-shortened ribbons suitable for imaging. SEM imaging of nanoribbons on a silicon surface shows that the ribbons remain long (, 4 mm in this image) when not cut by tip sonication; they can be dispersed as single or thin layers and they display uniform widths and predominantly straight edges over their entire length. The degree of consecutive tube opening in the MWCNTs can also be controlled by adjusting the amount of oxidizing agent introduced into the system; using TEM, we found that in 80–100% of the MWCNTs present, the side walls completely unravelled to form nanoribbons when 500 wt% KMnO4 was used. The successive opening reaction was demonstrated in five iterations, each containing a stepwise increase in the amount of KMnO4: 100 wt% KMnO4 in the first iteration (sample I), 200 wt% in the second iteration (sample II),and so on until the final iteration, when we used 500 wt%.

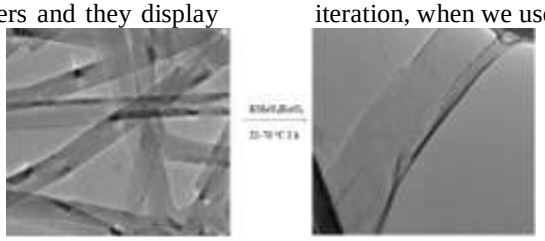

Figure:-3c,TEMimages depicting the transformation ofMWCNTs (left) into oxidized nanoribbons (right). The right-hand side of the ribbon is partly folded onto itself. The dark structures are part of the carbon imaging grid.

This resulted in consecutive unencapsulation of the different layers by unzipping of the successive MWCNTs (see Methods for details). Itis evident from TEM images (that the walls of the MWCNTs open to a higher degree as the level of oxidation increases, with lessMWCNTinner tube remaining in successive iterations. This is highlighted in a statistical plot showing the decrease of the average diameter of remaining MWCNTs from, 65nmto, 20nm as the amount of KMnO4 exposure is increased. The smallerdiameter tubes that remained after treatment with 500 wt%KMnO4 were exposed to the reaction conditions for less time than the larger-diameter tubes and, thus, may not have had the chance tofully react; no difference in the rate of unzipping between smallerand larger-diameter Nanotube can be inferred from this data.

Pre-oxidation

In pre-oxidation method the MWCNT was treated with concentrated sulphuric acid(H2SO4) and Nitric acid (HNO3) to enhance oxygen. MWCNT was suspended in a mixture of 50ml of H2SO4 and 25 ml of HNO3 for more than 12 hours. 50 ml of H2O was added to acceleratethe reaction. Next day stirring was done for 10 min. After 24 hours MWCNT was collected inthe bottom of beaker and washed with H2O for several times to remove acids. By help of a phpaper acidic nature was tested. Then solution was dried to collect CNT power.

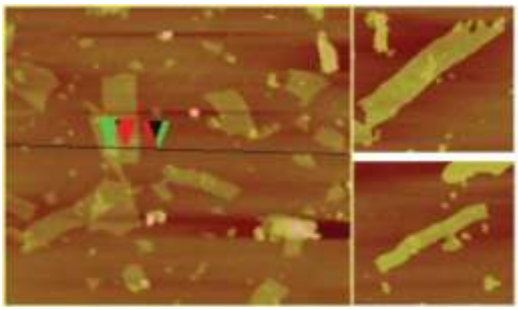

Figure:-3d,AFMimages of partly stacked multiple short fragments of nanoribbons that were horizontally cut by tip-ultrasonic treatment of the original oxidation productto facilitate spin-casting onto the mica surface. The height data (inset) indicates that the ribbons are generally single layered. The two small images on the right show some other characteristic nanoribbons.

International journal of advances in engineering and management (IJAEM)
Volume 3, issue 6 June 2021, pp: 1822-1832 www.ijaem.net ISSN: 2395-5252

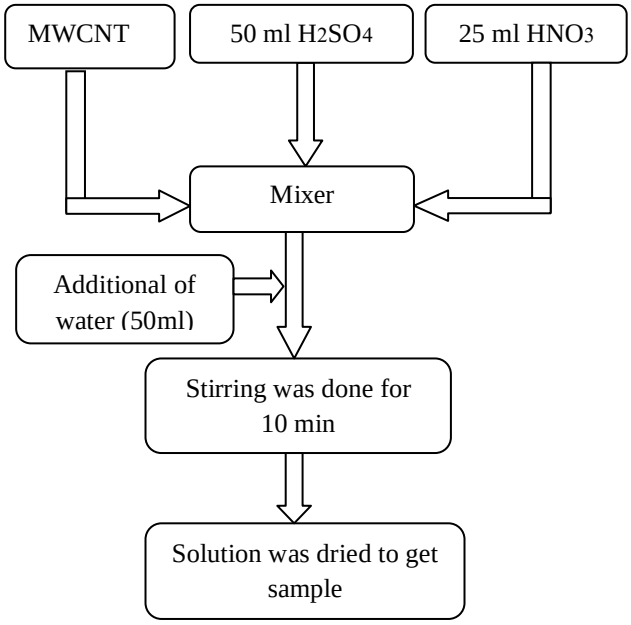

Figure:-4 preoxidation flow chart

Oxidation

MWCNT will be suspended in concentrated 50 ml of sulphuric acid (H2SO4) for a period of 1–12 h. Then solution was treated with 500 wt% potassium permanganate (KMnO4). The H2SO4 conditions aid in exfoliating the nanotube and the subsequent graphene structures. Thereaction mixture was stirred at room temperature for 1 h and then heat for 50–700C for anadditional 1 h. Now quenches the reaction mixture by pouring over ice containing a smallamount of hydrogen peroxide (H2O2). The solution was filter over a poly tetra fluoro-ethylene(PTFE) membrane, and the remaining solid to wash with de-ionized water. Then dried CNT was collected[46].

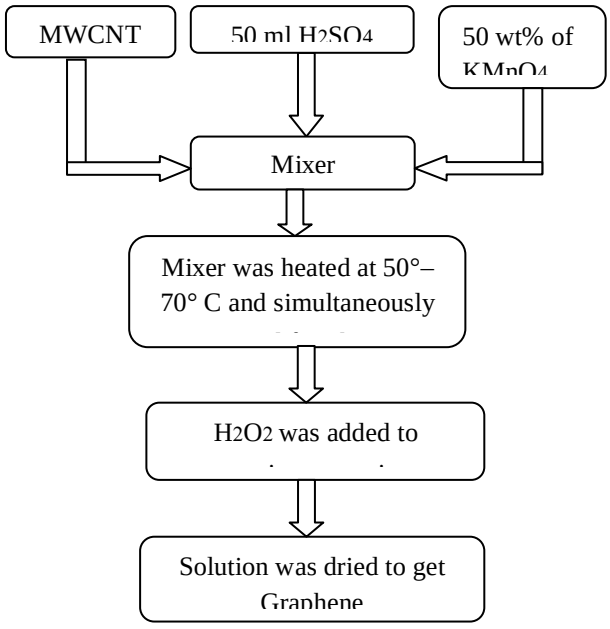

Figure:-5oxidation flow chart

International journal of advances in engineering and management (IJAEM)
Volume 3, issue 6 June 2021, pp: 1822-1832 www.ijaem.net ISSN: 2395-5252

Liquid Phase ExfoliationNanosheets

Graphene has attracted great interests during the past decade [47-49]. The excellent electrical and optical properties make it promising in a variety of devices such as high speed transistors [50-52], transparent conducing films [53,54], lithium ion batteries [55-57], and super capacitors [55,57,58]. Its electrical conductivity, which is largely affected by the presence of defects and functional groups, governs the performance of many of these devices [59]. Therefore, the preparation of graphene with low concentration of defects and functional groups is crucial for many of its applications. In addition, in view of industrial applications, high-yield production is also highly demanded.

Liquid-phase exfoliation has been considered as one of the most feasible approach for industrial production of graphene due to its scalability and low cost. This approach typically involves sonication of graphite or graphite oxide powders in solvents. Depending on the graphite precursors, liquid-phase exfoliation of graphite has been studied using (1) graphite oxide, (2) natural graphite, and (3) graphite intercalation compound (GIC).

Liquid-phase exfoliation of graphite oxide is now one of the most widely used methods for preparation of graphene. This method begins with intercalation of graphite with strong oxidizing agents followed by expansion of graphite layers via sonication. The reduction of the obtained graphene oxide to graphene is usually conducted by either thermal or chemical approaches [60,61]. Although this method is capable of high-yield (>50%) production of graphene, the use of large quantity of acid and oxidizing agents requires time-consuming washing steps and produces hazardous wastes. In addition, the vigorous oxidation of graphite often leads to incomplete restoration of the sp2 hybrid carbon bonds and presence of residual oxygen functional groups resulting in poor electrical conductance [62].

Liquid phase exfoliation of natural graphite is easy to implement and can circumvent the oxidation of graphene. This method involves ultrasonic treatment of graphite in solvents such as N-methyl-2-pyrrolidone (NMP), N'N-dimethylformamide (DMF), and γ-butyrolactone (GBL) [63]. Among all the solvents, NMP gives the highest graphene yield due to its surface energy approaching that of graphite that is sufficient to overcome the interacting forces between graphene layers. Although technically it is similar to the liquid-phase exfoliation of graphite oxide, this method is unique with the absence of oxidative intercalation steps. Graphene prepared by this method was demonstrated to have low concentration of defects and oxygen functional groups. However, the yield is usually very low (~1 wt %) as only the surface layers of graphite were peeled off during sonication.

Liquid-phase exfoliation of GICs for production of graphene was first reported by Viculis et al and has attracted great interest recently [64-67]. This method begins with intercalation of graphite followed by expansion of graphite via rapid increase in the vapor pressure of the volatile intercalated substance under microwave or thermal treatment. As nonoxidative agents are applied for intercalation of graphite and microwave or thermal treatment of GIC leads to large expansion of graphite, high-yield production of graphene with high quality can be achieved using this method. For example, it was reported that, by solvothermal-assisted exfoliation of expanded graphite (EG) obtained from GIC in acetonitrile, Qian et al. successfully prepared mololayer and bilayer graphene with 10-12 wt% yield without significant structural defects [68]. However, these recipes are limited by using either poisonous chemical agents [65] or dangerous chemical reactions [66,67].

Natural graphite (2 g, 99.99% purity) was first mixed with an aqueous solution (300 ml) containing TEA tetrafluoroborate (0.8 g), sodium hydroxide (0.15 g), and thionin acetate salt (50 mg). After agitation for 10 minutes, the suspension was tip sonicated for 6 hours (Scientz-II D Ultrasonic Cell Disruptor, 950 W, with 90% amplitude modulation) and then vacuum filtered by Nylon membrane of 220 nm in pore size. The obtained TEA-GIC was washed with 20 ml deionized water and 20 ml ethanol for three times successively and then vacuum dried at 60 °C for 2 hours. After that, the dry graphite powders were microwave irradiated for 5 minutes (Midea microwave oven, 900 W). The expanded graphite (EG) obtained by microwave treatment was then treated ultrasonically in 700 ml NMP for 2 hours (Ultrasonic Cleaner, 250 W). The resultant suspension containing graphene was centrifuged at 5000 rpm for 15 minutes to remove unexfoliated graphite particles. A stable graphene suspension was obtained finally after the supernatant was pipetted off.

REFERENCES

[1]. Lee, C., Wei, X., Kysar, J. W. & Hone, J. Measurement of the elastic properties and intrinsic strength of monolayer graphene. Science 321, 385–388 (2008).

[2]. Balandin, A. A. et al. Superior thermal conductivity of single-layer graphene. Nano Lett. 8, 902–907 (2008).
[3]. Bolotin, K. I. et al. Ultrahigh electron mobility in suspended graphene. Solid State Commun. 146, 351–355 (2008).
[4]. Stoller, M. D., Park, S., Zhu, Y., An, J. &Ruoff, R. S. Graphene-based ultracapacitors. Nano Lett. 8, 3498–3502 (2008).
[5]. Zhang, Y., Tan, Y.-W., Stormer, H. L. & Kim, P. Experimental observation of the quantum Hall effect and Berry's phase in graphene. Nature 438, 201–204 (2005).
[6]. Y.Zahang, Y.W.Tan, H.L.Stormer , P.kim,"Experimental observation of the quantum hall effect and berry 's phase in graphene " Nature , vol .438,pp.201-204 ,November 2005.
[7]. Kelly BT. Physics of graphite. London: applied science publication 1981.
[8]. Hot Technologies Challenges andOpportunitiesfor the MassProduction of HighQuality Graphene:An Analysis ofWorldwide Patents
[9]. K.S.Novoselov, A.K.Geim, S.V.Morozov, et al., Science, 306, 666 (2004).
[10]. A.K.Geim, K.S.Novoselov, Nature Mater., 6, 183 (2007).
[11]. A.C.Ferrari, Solid State Commun., 143, 47 (2007).
[12]. A.K.Geim, Science, 324, 1530 (2009).
[13]. A.H.CastroNeto, F.Guinea, N.M.R.Peres, et al., Rev. Mod. Phys., 81, 109 (2009).
[14]. A.Schwierz, Nat. Nanotech, 5, 487 (2010).
[15]. A.Ferrari,J.Meyer, V.Scardaci, C.Casiraghi, et al., Phys. Rev. Lett., 97, 1 (2006).
[16]. P.Blake, E.W.Hill, A.H Castro Neto, et al., Appl. Phys. Lett., 91, 063124 (2007).
[17]. C.Casiraghi, S.Pisana, K.S.Novoselov, A.K.Geim, A.C.Ferrari, Appl. Phys. Lett., 91, 233108 (2007).
[18]. S.Pisana, M.Lazzeri, C.Casiraghi, et al., Nature Materials, 6, 198 (2007).
[19]. A.Reina, X.Jia, J.Ho, D.Nezich, H.Son, V.Bulovic, M.S.Dresselhaus, J.Kong., Nano Letters, 9, 30(2009).
[20]. A.C.Ferrari, J.C.Meyer, V.Scardaci, C.Casiraghi, M.Lazzeri, F.Mauri, S.Piscanec, D.Jiang,K.S.Novoselov, S.Roth, A.K.Geim, Phys. Rev. Lett., 97, 187401 (2006).
[21]. R.F.Casten, N.V.Zamfir, P.Von Brentano, W.T.Chou, Phys. Rev. C, 45, R1413 (1992).
[22]. C.Casiraghi, A.Hartschuh, E.Lidorikis, et al., Nano Letters, 7, 9 (2007).
[23]. G.Shmavonyan, S.Giordani, G.Sevoyan, N.PesentiMaterials of the 3rd COST annual scientificmeeting, Designing novel materials for nanodevices: From Theory to Practice, Berlin, Germany,December 9-12, 2012.
[24]. Enlarging the surface area of monolayer Graphene synthesized by mechanical exfoliatg. sh. shmavonyan1, g.g. sevoyan1, v. m. aroutiounian2 armenian journal of physics, 2013, vol. 6, issue 1, pp. 1-6
[25]. A. Castellanos-Gomez, M. Barkelid, A. M. Goossens, et al., Nano Lett, 12, 1 (2012).
[26]. http://www.youngscientistjournal.org/2013/article/towards-fabrication-graphene-mos2-junction.
[27]. Geim, A. K. &Novoselov, K. S. The rise of graphene. Nature Mater. 6, 183–191 (2007).
[28]. Novoselov, K. S. et al. Two-dimensional gas of massless Dirac fermions in graphene. Nature 438, 197–200 (2005).
[29]. Zhang, Y., Tan, Y.-W., Stormer, H. L. & Kim, P. Experimental observation of the quantum Hall effect and Berry's phase in graphene. Nature 438, 201–204 (2005).
[30]. Areshkin, D. A., Gunlycke, D. & White, C. T. Ballistic transport in graphene nanostrips in the presence of disorder: importance of edge effects. Nano Lett. 7, 204–210 (2007).
[31]. Nakada, K., Fujita, M., Dresselhaus, G. &Dresselhaus, M. S. Edge state in graphene ribbons: nanometer size effect and edge shape dependence. Phys. Rev. B 54, 17954–17961 (1996).
[32]. Son, Y.-W., Cohen, M. L. &Louie, S. G. Energy gaps in graphene nanoribbons. Phys. Rev. Lett. 97, 216803 (2006).
[33]. [33] Han, M. Y., Oezyilmaz, B., Zhang, Y. & Kim, P. Energy band-gap engineering of graphene nanoribbons. Phys. Rev. Lett. 98, 206805 (2007).
[34]. Chen, Z., Lin, Y.-M., Rooks, M. J. &Avouris, P. Graphene nano-ribbon electronics. Physica E 40, 228–232 (2007).
[35]. Schniepp, H. C. et al. functionalized single graphene sheets derived from splitting graphite oxide. J. Phys. Chem. B 110, 8535–8539 (2006).
[36]. Rollings, E. et al. Synthesis and characterization of atomically thin graphite films on a silicon carbide substrate. J. Phys. Chem. Solids 67, 2172–2177 (2006).
[37]. Li, X., Wang, X., Zhang, L., Lee, S. & Dai, H. Chemically derived, ultrasmooth graphene nanoribbon semiconductors. Science 319, 1229–1232 (2008).

[38]. Yang, X. et al. Two-dimensional graphene nanoribbons. J. Am. Chem. Soc. 130, 4216–4217 (2008).
[39]. Campos-Delgado, J. et al. Bulk production of a new form of sp2 carbon: crystalline graphene nanoribbons. Nano Lett. 8, 2773–2778 (2008).
[40]. Saito, T., Matsushige, K. & Tanaka, K. Chemical treatment and modification of multi-walled carbon nanotubes. Physica B 323, 280–283 (2002).
[41]. Son, Y.-W., Cohen, M. L. & Louie, S. G. Half-metallic graphene nanoribbons. Nature 444, 347–349 (2006).
[42]. Liang, G., Neophytou, N., Nikonov, D. E. &Lundstrom, M. S. Performance projections for ballistic graphene nanoribbon field-effect transistors. IEEE Trans. Electron. Dev. 54, 677–682 (2007).
[43]. Wang, X. et al. Room-temperature all-semiconducting sub-10-nm graphene nanoribbon field-effect transistors. Phys. Rev. Lett. 100, 206803 (2008).
[44]. Wolfe, S., Ingold, C. F. & Lemieux, R. U. Oxidation of olefins by potassium permanganate: mechanismofa-ketol formation. J.Am. Chem. Soc. 103,938–939(1981).
[45]. Banoo, F. & Stewart, R. Mechanisms of permanganate oxidation. IX. Permanganate oxidation of aromatic alcohols in acid solution. Can. J. Chem. 47, 3199–3205 (1969).
[46]. Vol 458 16 April 2009doi: 10.1038/nature07872 Stankovich, S. et al. Synthesis of graphene-based nano-sheets via chemical metod.
[47]. A.K. Geim and K.S. Novoselov, Nature Mater., 6 (2007) 183.
[48]. Y.W. Zhu, S. Murali, W.W. Cai, X.S. Li, J.W. Suk, J.R. Potts and R.S. Ruoff, Adv. Mater., 22 (2010) 3906.
[49]. M.J. Allen, V.C. Tung and R.B. Kaner, Chem. Rev., 110 (2010) 132.
[50]. F. Schwierz, Nature Nanotechnol., 5 (2010) 487.
[51]. P. Avouris, Z.H. Chen and V. Perebeinos, Nature Nanotechnol., 2 (2007) 605.
[52]. M. Burghard, H. Klauk and K. Kern, Adv. Mater., 21 (2009) 2586.
[53]. S. Roth and H.J. Park, Chem. Soc. Rev., 39 (2010) 2477.
[54]. F. Bonaccorso, Z. Sun, T. Hason and A.C. Ferrari, Nature Photonics, 4 (2010) 611.
[55]. M.H. Liang, B. Luo and L.J. Zhi, Inter. J. Energy Res., 33 (2009) 1161.
[56]. F. Han, A.H. Lu and C.W. Li, Prog. Chem., 24 (2012) 2443.
[57]. J. Liu, Y.H. Xue, M. Zhang and L.M. Dai, MRS Bull., 37 (2012) 1265.
[58]. L.L. Zhang, R. Zhou and X.S. Zhao, J. Mater. Chem., 20 (2010) 5983.
[59]. N.M.R. Peres, F. Guinea and A.H.C. Neto, Phys. Rev., B 73 (2006) 125411.
[60]. Y. Xu, H. Bai, G. Lu, C. Li and G. Shi, J. Am. Chem. Soc., 130 (2008) 5856.
[61]. S. Stankovich, D.A. Dikin, R.D. Piner, K.A. Kohlhaas, A. Kleinhammes A, Y.Y. Jia, Y. Wu, S.T. Nguyen and R.S. Ruoff, Carbon, 45 (2007) 1558.
[62]. S. Park and R.S. Ruoff, Nature Nanotechnol., 4 (2009) 217.
[63]. Y. Hernandez , V. Nicolosi, M. Lotya, F.M. Blighe, Z. Sun, S. De, T.T. McGovern, B. Holland, M. Byrne, Y.K. Gun'ko, J.J. Boland, P. Nuraj, G. Duesberg, S. Krishnamurthy, R. Goodhue, J. Hutchison, V. Scardaci, A.C. Ferrari and J.N. Coleman, Nature Nanotechnol., 3 (2008) 563.
[64]. L.M. Virculis, J.J. Mack, O.M. Mayer, H.T. Hahn and R.B. Kaner, J. Mater. Chem., 15 (2005) 974.
[65]. J.H. Lee, D.W. Shin, V.G. Makotchenko, A.S. Nazarov, V.E. Fedorov, Y.H. Kim, J.Y. Choi, J.M. Kim and J.B. Yoo, Adv. Chem., 21 (2009) 4383.
[66]. W.T. Gu, W. Zhang, X.M. Li, H.W. Zhu, J.Q. Wei, Z. Li, Q. Shu, C. Wang, K.L. Wang, W. Shen, F.Y. Kang and D.H. Wu, J. Mater. Chem., 19 (2009) 3367.
[67]. E.H.L. Falcao, R.G. Blair, J.J. Mack, L.M. Viculis, C.W. Kwon, M. Bendikov, R.B. Kaner and B.S. Dunn, Carbon, 45 (2007) 1367.